



Predictive value of longitudinal systemic inflammatory markers for pathologic response to neoadjuvant PD-1 blockade in resectable non-small cell lung cancer

Xiuli Tao^{1#}, Qian Zhang^{2#}, Pei Yuan³, Shuhang Wang⁴, Jianming Ying³, Ning Li⁴, Wei Guo⁵, Jing Li^{1,2}, Lei Guo³, Ying Liu¹, Zewei Zhang¹, Shijun Zhao², Shugeng Gao⁵, Ning Wu^{1,2}

¹Department of Nuclear Medicine (PET-CT Center), National Cancer Center/National Clinical Research Center for Cancer/Cancer Hospital, Chinese Academy of Medical Sciences and Peking Union Medical College, Beijing, China; ²Department of Diagnostic Radiology, National Cancer Center/National Clinical Research Center for Cancer/Cancer Hospital, Chinese Academy of Medical Sciences and Peking Union Medical College, Beijing, China; ³Department of Pathology, National Cancer Center/National Clinical Research Center for Cancer/Cancer Hospital, Chinese Academy of Medical Sciences and Peking Union Medical College, Beijing, China; ⁴Department of Clinical Trial Center, National Cancer Center/National Clinical Research Center for Cancer/Cancer Hospital, Chinese Academy of Medical Sciences and Peking Union Medical College, Beijing, China; ⁵Department of Thoracic Surgery, National Cancer Center/National Clinical Research Center for Cancer/Cancer Hospital, Chinese Academy of Medical Sciences and Peking Union Medical College, Beijing, China

Contributions: (I) Conception and design: X Tao, Q Zhang, S Gao, N Wu; (II) Administrative support: J Ying, N Li, S Gao, N Wu; (III) Provision of study materials or patients: X Tao, S Wang, W Guo; (IV) Collection and assembly of data: X Tao, Q Zhang, P Yuan, Z Zhang; (V) Data analysis and interpretation: X Tao, Q Zhang, P Yuan, J Li, L Guo, Y Liu, Z Zhang, S Zhao; (VI) Manuscript writing: All authors; (VII) Final approval of manuscript: All authors.

[#]These authors contributed equally to this work as co-first authors.

Correspondence to: Ning Wu, MD. Department of Nuclear Medicine (PET-CT Center), National Cancer Center/National Clinical Research Center for Cancer/Cancer Hospital, Chinese Academy of Medical Sciences and Peking Union Medical College, No. 17, Panjiayuan Nanli, Beijing 100021, China; Department of Diagnostic Radiology, National Cancer Center/National Clinical Research Center for Cancer/Cancer Hospital, Chinese Academy of Medical Sciences and Peking Union Medical College, Beijing, China. Email: cjr.wuning@vip.163.com; Shugeng Gao, MD. Department of Thoracic Surgery, National Cancer Center/National Clinical Research Center for Cancer/Cancer Hospital, Chinese Academy of Medical Sciences and Peking Union Medical College, No. 17 Panjiayuan Nanli, Beijing 100021, China. Email: gaoshugeng@cicams.ac.cn.

Background: Identifying biomarkers to predict responses for neoadjuvant immunotherapy in resectable non-small cell lung cancer (NSCLC) is under intensive study. Considering the interplay between cancer, inflammation, and immunosuppression, we hypothesized that circulating and imaging inflammatory markers could serve as indicators of anti-tumor immune responses, and thus conducting an exploratory study to reveal the predictive value of combining longitudinal systemic inflammatory markers in stratifying pathologic response to neoadjuvant sintilimab.

Methods: We retrospectively reviewed 36 patients (29 male and seven female) with NSCLC (stage IA–IIIB) who underwent pre- and post-treatment peripheral blood tests and ¹⁸F-fluorodeoxyglucose positron emission tomography/computed tomography (¹⁸F-FDG PET/CT) scans before and after two cycles of neoadjuvant sintilimab (registration number: ChiCTR-OIC-17013726). The neutrophil-to-lymphocyte ratio (NLR), immune-related adverse events (irAEs) on imaging, and lymphoid organ metabolism [spleen-to-liver ratio (SLR) and bone marrow-to-liver ratio (BLR)] were evaluated to examine their predictive value for the major pathologic response (MPR). Significant variables were used to classify patients into low, intermediate, and high inflammatory burden groups for stratifying pathologic regression and tumor-infiltrating immune cells abundance in the tumor microenvironment. Spearman's correlation analysis was performed to explore the correlation between systemic inflammatory markers, primary tumor metabolism, and tumor-infiltrating immune cells abundance at various time points.

Results: Of the 36 enrolled patients, 13 (36.1%) exhibited MPR. Δ NLR% was a significant negative predictor of MPR ($P=0.047$) and negatively correlated with pathologic regression ($r=-0.34$, $P=0.045$). Pre-

and post-treatment SLRs were potential negative predictors of MPR ($P=0.06$; $P=0.055$) and negatively correlated with pathologic regression ($r=-0.30$, $P=0.07$; $r=-0.31$, $P=0.06$). The high inflammatory burden group (pre-treatment SLR >0.83 and $\Delta\text{NLR}\% >-17\%$) had the lowest pathologic regression ($P=0.01$) and the highest infiltration abundance of pre-treatment CD68⁺ macrophage ($P=0.01-0.04$). irAEs on imaging did not have significant effects on MPR and pathologic regression in overall and per-organ analyses.

Conclusions: The combination of pre-treatment SLR and $\Delta\text{NLR}\%$ demonstrates predictive value in stratifying pathologic response to neoadjuvant immunotherapy in resectable NSCLC. The high inflammatory burden group had the lowest pathologic regression and the pre-treatment immunosuppressive microenvironment with macrophage enrichment.

Keywords: Non-small cell lung cancer (NSCLC); neoadjuvant immunotherapy; neutrophil-to-lymphocyte ratio (NLR); ¹⁸F-fluorodeoxyglucose positron emission tomography/computed tomography (¹⁸F-FDG PET/CT); tumor microenvironment

Submitted Jul 12, 2024. Accepted for publication Oct 12, 2024. Published online Nov 28, 2024.

doi: 10.21037/tlcr-24-598

View this article at: <https://dx.doi.org/10.21037/tlcr-24-598>

Introduction

Lung cancer, particularly non-small cell lung cancer (NSCLC), is the most common cause of cancer-related death worldwide (1). In recent years, clinical trials on neoadjuvant immunotherapy for resectable NSCLC have been conducted with encouraging results (2-5), but not all patients responded satisfactorily. The major pathologic response (MPR) is considered as a vital short-term endpoint that has potential to replace survival outcomes in neoadjuvant immunotherapy setting. Identification of biomarkers to predict responses has become an area of intensive researches.

The links among cancer, inflammation, and immunosuppression are well recognised (6), and cancer-related inflammation plays a key role in tumor progression (7-9). A few studies have reported that a high systemic inflammatory burden is associated with poor efficacy and prognosis (10-13), whereas immune activation is associated with better efficacy and prognosis (14,15). However, the role of inflammatory markers in neoadjuvant immunotherapy remains inconclusive. In addition, tumor-infiltrating immune cells within the tumor immune microenvironment (TIME) play important roles in anti-tumor immunity, particularly CD8⁺ T cell (16). However, overall and dynamic detection of TIME biomarkers remains challenging.

We have previously demonstrated that metabolic

parameters of primary tumor can predict MPR to neoadjuvant sintilimab in resectable NSCLC (17). Considering the interplay between cancer, inflammation, and immunosuppression, we further conducted an exploratory study to reveal the predictive value of combining longitudinal systemic inflammatory markers in stratifying pathologic response. We hypothesised that circulating and imaging inflammatory markers would serve as indicators for the anti-tumor immune responses. Peripheral blood tests and ¹⁸F-fluorodeoxyglucose (¹⁸F-FDG) positron emission tomography/computed tomography (PET/CT) scans were used to assess the systemic inflammatory burden. Notably, as peripheral blood is susceptible to infection and other factors, we focused on the combined effect of lymphoid organs metabolism (spleen and bone marrow) to comprehensively reflect the systemic inflammatory burden of the host.

Based on peripheral blood tests and ¹⁸F-FDG PET/CT scans, the objective of this study was to explore the predictive value of longitudinal systemic inflammatory markers to stratify the pathologic response to resectable NSCLC in neoadjuvant immunotherapy setting. Moreover, we explored the relationship between systemic inflammatory markers and tumor-infiltrating immune cells to provide potential non-invasive surrogate markers for TIME information. We present this article in accordance with the TRIPOD reporting checklist (available at <https://tlcr.amegroups.com/article/view/10.21037/tlcr-24-598/rc>).

Methods

Data source

Patients were selected from a prospective, single-center, single-arm, phase Ib trial (registration number: ChiCTR-OIC-17013726). From March 6, 2018 to March 8, 2019, a total of 40 patients with resectable NSCLC were enrolled in the trial and 36 patients who underwent pre- and post-treatment peripheral blood tests and ^{18}F -FDG PET/CT scans before and after two cycles of neoadjuvant sintilimab were enrolled in this study. Four patients were excluded: two of them for the baseline PET/CT which was conducted in other hospital, and two of them for the pathologic regression of primary tumor that could not be assessed by the exploratory surgery. Eligible patients were those aged 18–75 years who had histologically or cytologically confirmed NSCLC [stage IA–IIIB, American Joint Committee on Cancer (AJCC) 8th] that was surgically resectable. All patients were treatment-naïve and had a

primary tumor with diameter ≥ 2 cm. The exclusion criteria were previous anti-tumor therapy; epidermal growth factor receptor-sensitive mutation; systemic immunosuppressive therapy within 4 weeks prior to study treatment; active and uncontrolled infection; history of interstitial lung disease; known or suspected active autoimmune diseases; hypersensitivity to any monoclonal antibodies; and presence of other known malignant tumor. The complete eligibility criteria (inclusion and exclusion criteria) were available in our previous publications (3,17). The eligible patients received two cycles of sintilimab (200 mg, intravenously, day 1 and 22), and complete tumor resection or biopsy (to confirm tumor progression) was performed for pathological evaluation within 29–43 days after the first dose. Data were extracted from the medical records.

The study was conducted in accordance with the Declaration of Helsinki (as revised in 2013) and was approved by the Ethics Committee and Institutional Review Board of the National Cancer Center/Cancer Hospital, Chinese Academy of Medical Sciences and Peking Union Medical College (No. 17-151/1407). Written informed consent was obtained from all patients.

Highlight box

Key findings

- This study proposed that combined systemic inflammatory markers demonstrated predictive value in stratifying pathologic response to neoadjuvant sintilimab in resectable non-small cell lung cancer (NSCLC). The high inflammatory burden group had the lowest pathologic regression and the pre-treatment immunosuppressive microenvironment with macrophage enrichment.

What is known and what is new?

- Cancer-related inflammation plays a key role in tumor progression. A few studies have reported that patients with high systemic inflammatory burden are associated with poor efficacy and prognosis.
- Based on the hypothesis that circulating and imaging inflammatory markers could serve as indicators for the anti-tumor immune responses, we reported the predictive value of longitudinal systemic inflammatory markers for pathologic response to resectable NSCLC in the neoadjuvant immunotherapy setting, and explored the relationship between host inflammatory burden and tumor-infiltrating immune cells in the microenvironment.

What is the implication, and what should change now?

- Longitudinal systemic inflammatory markers from peripheral blood and positron emission tomography/computed tomography can stratify pathologic response to resectable NSCLC in neoadjuvant immunotherapy setting, assisting in patients selection with potential benefits. Our findings serve as preliminary data to encourage prospective studies to further explore the pathophysiological mechanisms involving systemic inflammatory markers and their association with the tumor immune microenvironment and clinical outcomes.

^{18}F -FDG PET/CT acquisition

Three-dimensional (3D) whole-body PET/CT scans from head to thigh were performed using an integrated PET/CT device (Discovery 690; GE Healthcare, Milwaukee, Wisconsin, USA), according to the standard protocol. Prior to the scan, the patients fasted for at least 6 h, and the blood glucose level was required to be <145 mg/dL. PET/CT scans were acquired approximately 50–70 min after intravenous administration of ^{18}F -FDG at a mean dose of 3.70–4.44 MBq/kg. The difference in the administration dose was $<20\%$, and the difference in uptake time was <15 min between the pre- and post-treatment PET/CT scans. PET images were obtained in 3D image-acquisition mode using 2 min per frame (generally 7–8 beds location) and reconstructed using the VPFX-S algorithm (two iterations, 24 subsets, 4 mm Gaussian post-filter). Spiral CT was performed using a standardised protocol (tube voltage, 120 kV; tube current, 150 mA; slice thickness, 3.75 mm; and rotation speed, 0.8 s) without intravenous contrast administration. A breath-hold thoracic spiral CT scan (tube voltage, 120 kV; tube current using the automatic milliamperes-seconds technology; slice thickness, 5 mm; and rotation speed, 0.5 s) was performed after the PET/CT scan with image reconstruction (slice thickness, 1.25 mm;

space, 0.8 mm).

Image analysis

The PET/CT images were retrospectively assessed and interpreted by two radiologists who were blinded to clinical data. Disagreements were resolved through consensus. PET/CT images were analysed using PETVCAR (PET Volume Computerized Assisted Reporting), an automated segmentation software system with an iterative adaptive algorithm for detecting the threshold levels on an advantage workstation (version 4.6; GE Healthcare).

Inflammatory markers in spleen and bone marrow metabolism

Spleen and bone marrow metabolism were normalized by computing the spleen-to-liver ratio (SLR) and the bone marrow-to-liver ratio (BLR), respectively. Prigent *et al.* (18) reported the interobserver variability and confirmed that the robust metrics with strong reproducibility were the mean standardized uptake value (SUV) of the spleen and bone marrow measurements (SLR_{mean} and BLR_{mean}). Therefore, the SLR and BLR were calculated by dividing the spleen SUV_{mean} by the liver SUV_{mean} and the bone marrow SUV_{mean} by liver SUV_{mean}, respectively. The measurement methods of volume of interest (VOI) were consistent with previous studies (Figure S1) (18-20). The SUV_{mean} of the liver and spleen were computed from a spherical VOI 30 mm in diameter on the right liver lobe and a spherical VOI 20 mm in diameter at the center of the spleen. For the bone marrow, four spherical VOIs of 15 mm diameter were placed in the center of the L1 to L4 (lumbar) vertebral bodies, whereas VOIs with vertebral fractures, severe lumbar osteoarthritis, metastatic lesions, hemangiomas, or history of lumbar spine surgery were excluded. The SUV_{mean} of the bone marrow was defined as the average SUV_{mean} of all the vertebral bodies.

Metabolic tumor burden of the primary tumor

The VOI of the primary tumor was auto-contoured and segmented using a 3D cube that contained all FDG PET-positive areas and excluded negative normal tissues in the axial, coronal, and sagittal planes. The following SUVs corrected by lean body mass (SUL) were calculated: SUL_{max}, SUL_{mean}, SUL_{peak}, metabolic tumor volume (MTV), and total lesion glycolysis (TLG). Detailed information was available in our previous publication (17).

Immune-related adverse events (irAEs) detected on PET/CT

irAEs on PET/CT were visually defined as a diffuse and homogeneous increase in organ uptake that was newly emerging or markedly increased compared to the baseline image, or an increase in organ uptake that was quantitatively assessed (SUV_{peak} increase >30%) compared to the baseline image, which was consistent with the definition from a previous study (21). Diffuse inflammatory uptake of FDG for each organ (pneumonitis, thyroiditis, mediastinal granulomatous reaction, gastritis, colitis, hepatitis, pancreatitis, osteoarticular inflammation, cutaneous inflammation, pleuritis, etc.) was collected separately. Notably, there was no correspondence between clinically reported irAEs and irAEs on PET/CT. Clinical irAEs were not the focus of this study.

Inflammatory markers in peripheral blood

Complete blood cell counts were centrally tested in our institutional laboratory in accordance with standardized operative procedures. Records were obtained from the reports. Absolute neutrophil and lymphocyte counts were collected. The neutrophil-to-lymphocyte ratio (NLR) was calculated as the ratio of the absolute neutrophil count to the absolute lymphocyte count.

Pathological assessment

Routine hematoxylin and eosin staining were performed to assess the percentage of viable residual tumors in the primary tumor. The method for assessing pathologic responses was described in our previous publication (22). The degree of pathologic regression was recorded. Tumors with ≤10% viable tumor cells were considered to achieve MPR.

Detection of tumor-infiltrating immune cells

Multiplex immunofluorescence (mIF) staining was used to detect tumor-infiltrating immune cells. The slides were scanned using a PerkinElmer Vectra imaging system (Vectra 3.0.5; PerkinElmer, Waltham, Massachusetts, USA). The images of tissues stained separately with each reagent were used to construct spectral libraries, and the multispectral images were unmixed by the spectral libraries using the inForm Advanced Image Analysis software (inForm 2.3.0; PerkinElmer). The total infiltration abundance of immune

Table 1 Patients' characteristics (n=36)

| Clinical characteristics | Median [range]/n (%) |
|---|----------------------|
| Age (years) | 61 [48–70] |
| Sex | |
| Male | 29 (80.6) |
| Female | 7 (19.4) |
| Histology | |
| Adenocarcinoma | 6 (16.7) |
| Squamous cell carcinoma | 29 (80.6) |
| Mixed | 1 (2.8) |
| Smoking history | |
| Never | 8 (22.2) |
| Former or current | 28 (77.8) |
| Pack-years | 25 [0–100] |
| Clinical stage at baseline [†] | |
| Ia | 1 (2.8) |
| Ib | 6 (16.7) |
| IIb | 12 (33.3) |
| IIIa | 9 (25.0) |
| IIIb | 8 (22.2) |

[†], the clinical stage at baseline was based on the criteria of the American Joint Committee on Cancer, eighth edition.

cells (percentage of positively stained immune cells) was calculated by dividing the number of positively stained cells by the total number of nuclear cells. The detailed protocol for the mIF staining assay and data on the total region infiltration abundance of immune cells were available in our previous publication (23). Owing to insufficient adhesion causing samples to fall off the slide, among the 36 patients enrolled in the study, paired staining data from pre- and post-neoadjuvant therapy were available for 26 patients in the panel (CD8, PD-1), 23 patients in the panel (CD4, FOXP3), and 23 patients in the panel (CD56, CD19, CD68, CD163).

Statistical analysis

The variation was defined as the percentage change from pre- to post-neoadjuvant sintilimab. The calculation formula is as follows: the variation = $(X_{\text{Post}} - X_{\text{Pre}})/X_{\text{Pre}} \times 100\%$. Comparisons between MPR and non-MPR patients

were evaluated using Fisher's exact test for categorical variables and the Mann-Whitney *U* test for continuous variables. The predictive value of systemic inflammatory markers for MPR was calculated using receiver operating characteristic (ROC) analysis. The area under the ROC curve (AUC), sensitivity, specificity, and accuracy were calculated. Moreover, significant variables divided patients into three groups (low, intermediate, and high inflammatory burden groups). The Kruskal-Wallis test was used to compare differences in pathologic regression and pre-treatment infiltration abundance of tumor-infiltrating immune cells among the three groups. A *post-hoc* test with Bonferroni correction was performed for multiple comparisons.

The correlation between systemic inflammatory markers, primary tumor metabolism, and tumor-infiltrating immune cells abundance at various time points (pre-treatment, post-treatment, and variation) was determined using Spearman's correlation analysis. Available case analyses were used for the missing data.

Statistical analyses were performed using SPSS (version 25.0; IBM Corp.) and R (version 4.0.3). All reported P values were two-sided, and P values <0.05 were considered statistically significant. Considering the preliminary and exploratory nature of the study with its small sample size, the data obtained should be interpreted with caution and regarded as hypothesis-generating.

Results

Clinical characteristics of the patients

Among the 36 enrolled patients (29 male and 7 female; median age, 61 years), 35 patients underwent radical resection of the primary tumor after neoadjuvant sintilimab with different degrees of pathologic regression. None of the 35 patients had distant metastases. Only one patient did not undergo primary tumor resection, and was confirmed tumor progression by pleural biopsy of a new metastasis with the pathologic regression considered as 0. The median pathologic regression rate for all enrolled patients was 42.5% (0–100%). Overall, 36.1% (13/36) patients achieved MPR and 63.9% (23/36) patients did not achieve MPR. The patient characteristics are summarized in *Table 1*, and the study flowchart is presented in *Figure 1*. Descriptive statistics on the distribution and variation of systemic inflammatory markers and primary tumor metabolism before and after neoadjuvant sintilimab were detailed in

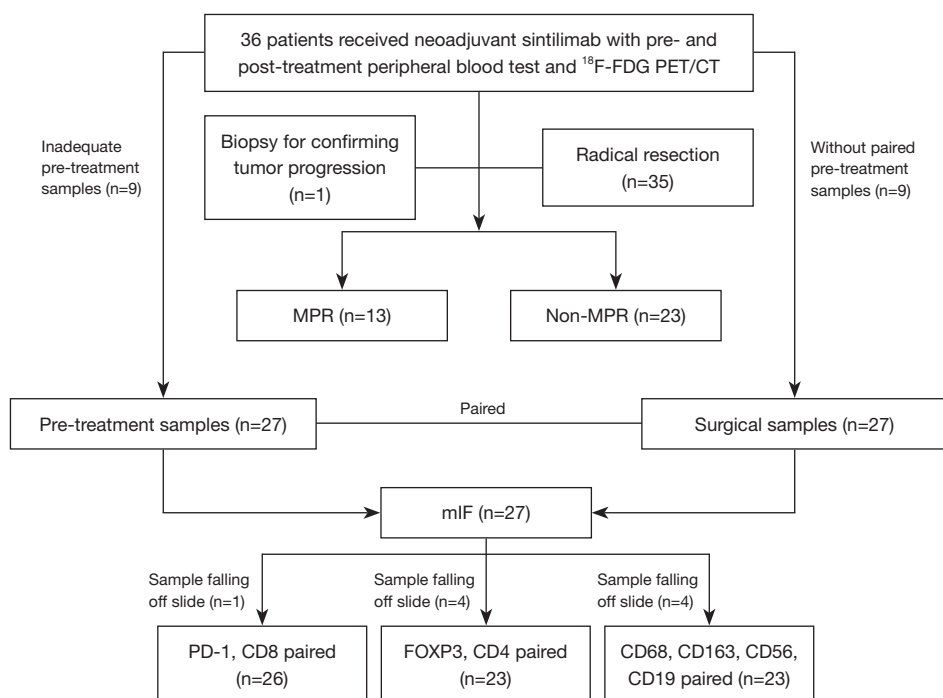


Figure 1 Study flowchart. ^{18}F -FDG PET/CT, ^{18}F -fluorodeoxyglucose positron emission tomography/computed tomography; MPR, major pathologic response; mIF, multiplex immunofluorescence.

Figure S2. According to our previous study, there was no significant correlation between the baseline characteristics of the patients in terms of age, sex, histology, smoking history, clinical stage, and MPR (17).

$\Delta\text{NLR}\%$ and pre- and post-treatment SLRs correlate with both MPR and pathologic regression

The relationship between pre- and post-treatment systemic inflammatory markers and pathologic responses is summarized in *Table 2* and *Table S1*. The $\Delta\text{NLR}\%$ in the MPR group was significantly lower than that in the non-MPR group ($P=0.047$). The $\Delta\text{NLR}\%$ was significantly negatively correlated with pathologic regression ($r=-0.34$, $P=0.045$). Further analyses indicated that the dominant significant effect was attributable to the absolute neutrophil count ($\Delta\%$). The absolute neutrophil count ($\Delta\%$) had significant effects on both MPR and pathologic regression (both $P=0.03$; *Tables S2,S3*). The pre- and post-treatment SLRs in patients with MPR tended to be significantly lower than those in patients without MPR, which almost reached significance ($P=0.06$; $P=0.055$). The pre- and post-treatment SLRs tended to be negatively correlated with pathologic

regression, which almost reached significance ($r=-0.30$, $P=0.07$; $r=-0.31$, $P=0.06$).

ROC analyses indicated that the $\Delta\text{NLR}\%$ (AUC =0.702), pre-treatment SLR (AUC =0.689), and post-treatment SLR (AUC =0.694) exhibited the best differentiation ability for MPR at thresholds of -17% , 0.83 , and 0.88 , respectively (*Table 3*). Significant variables with convenient integration into clinical routines ($\Delta\text{NLR}\%$ and pre-treatment SLR) divided patients into three groups. Considering the significant collinearity between pre- and post-treatment SLRs, the post-treatment SLR was not included in the classification. Patients were divided into three groups as follows: (I) the low inflammatory burden group (pre-treatment SLR ≤ 0.83 and $\Delta\text{NLR}\% \leq -17\%$); (II) the intermediate inflammatory burden group (pre-treatment SLR ≤ 0.83 and $\Delta\text{NLR}\% > -17\%$; pre-treatment SLR > 0.83 and $\Delta\text{NLR}\% \leq -17\%$); and (III) the high inflammatory burden group (pre-treatment SLR > 0.83 and $\Delta\text{NLR}\% > -17\%$). As shown in *Figure 2A*, there were significant differences in pathologic regression among the three groups ($P=0.01$). The high inflammatory burden group exhibited significantly lower pathologic regression than the low inflammatory burden group ($P=0.009$).

Table 2 Characteristics of systemic inflammatory markers with MPR

| Systemic inflammatory markers | Patients with MPR (n=13), median [range] | Patients without MPR (n=23), median [range] | P value |
|-------------------------------------|---|--|---------|
| Pre-treatment | | | |
| NLR | 2.9 [1.5, 6.6] | 2.8 [1.0, 10.3] | >0.99 |
| SLR | 0.8 [0.7, 1.1] | 0.9 [0.7, 1.3] | 0.06 |
| BLR | 0.8 [0.6, 1.6] | 0.9 [0.4, 2.3] | 0.18 |
| Post-treatment | | | |
| NLR | 2.1 [0.9, 4.2] | 2.3 [1.2, 12.0] | 0.23 |
| SLR | 0.8 [0.7, 0.9] | 0.9 [0.5, 1.1] | 0.055 |
| BLR | 0.8 [0.6, 0.9] | 0.8 [0.5, 2.4] | 0.33 |
| Percentage variation ($\Delta\%$) | | | |
| Δ NLR% | -22.7 [-74.6, 33.0] | -8.0 [-60.3, 224.5] | 0.047 |
| Δ SLR% | 0.1 [-27.6, 9.8] | -1.1 [-38.8, 19.4] | 0.95 |
| Δ BLR% | -4.9 [-42.3, 46.2] | -5.8 [-44.2, 47.7] | 0.63 |

MPR, major pathologic response; NLR, neutrophil-to-lymphocyte ratio; SLR, spleen-to-liver ratio; BLR, bone marrow-to-liver ratio.

Table 3 Diagnostic performance of systemic inflammatory markers for MPR

| Systemic inflammatory markers | Threshold | AUC (95% CI) | Sensitivity | Specificity | Accuracy | P value |
|-------------------------------|-----------|---------------------|-------------|-------------|----------|---------|
| Δ NLR% | -17 | 0.702 (0.529–0.876) | 0.692 | 0.696 | 0.694 | 0.046 |
| Pre-treatment SLR | 0.83 | 0.689 (0.496–0.882) | 0.615 | 0.783 | 0.722 | 0.06 |
| Post-treatment SLR | 0.88 | 0.694 (0.522–0.866) | 0.846 | 0.565 | 0.667 | 0.056 |

MPR, major pathologic response; AUC, area under the receiver operating characteristic curve; CI, confidence interval; NLR, neutrophil-to-lymphocyte ratio; SLR, spleen-to-liver ratio.

Evaluation of tumor-infiltrating immune cells in the TIME

We sought to determine whether pre-treatment tumor-infiltrating immune cells in the TIME differed among the three groups. As shown in *Figure 2B*, the infiltration abundance of macrophages ($CD68^+$, $CD68^+CD163^+$, and $CD68^+CD163^-$) differed significantly among the three groups ($P=0.01-0.04$). In particular, the infiltration abundance of macrophages ($CD68^+$, $CD68^+CD163^+$, and $CD68^+CD163^-$) was significantly higher in the high than in the low inflammatory burden group. There were no significant differences in the infiltration of $CD8^+$ T cells, $CD4^+$ T cells, $CD19^+$ B cells, and $CD56^+$ NK cells among the three groups. *Figure 3* showed the representative PET/CT and pre-treatment CD68 staining images of patients with the low and high inflammatory burden.

Subsequently, we explored the correlation of tumor-infiltrating immune cells abundance with systemic inflammatory markers and primary tumor metabolism at various time points (pre-treatment, post-treatment, and variation). As shown in *Figure 4*, the post-treatment SLR showed a significant positive correlation with $CD68^+$ and $CD68^+CD163^-$ macrophages ($r=0.53$ and 0.52 , $P=0.009$ and 0.01). The Δ BLR% was significantly negatively correlated with Δ CD19⁺ B cells ($r=-0.63$, $P=0.001$). The Δ SUL_{mean}% was significantly negatively correlated with Δ CD8⁺ and Δ CD8⁺PD1⁻ T cells ($r=-0.40$ and -0.42 , $P=0.04$ and 0.03).

Correlations between systemic inflammatory markers and primary tumor metabolism

The correlations between systemic inflammatory markers

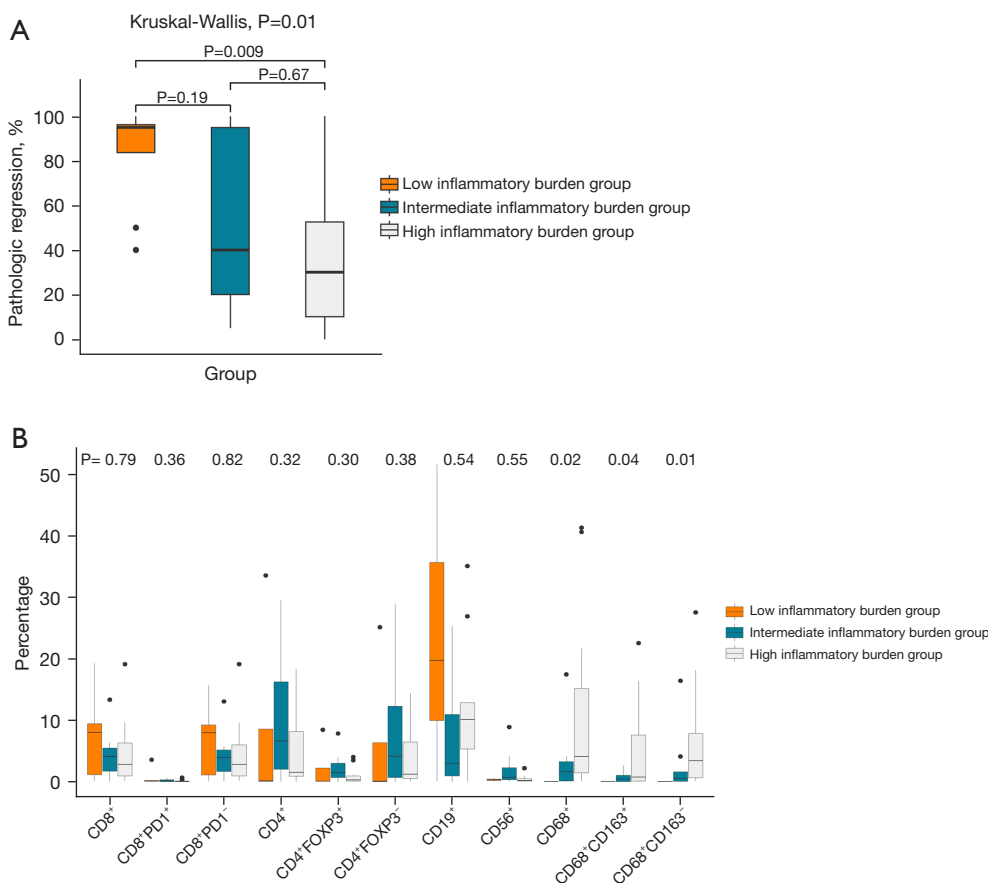


Figure 2 Comparison of pathologic regression and pre-treatment tumor-infiltrating immune cells abundance among the low, intermediate, and high inflammatory burden groups. (A) Comparison of pathologic regression to neoadjuvant immunotherapy among three groups. (B) Comparison of pre-treatment tumor-infiltrating immune cells abundance among three groups. In the boxplots, the center line represents the median value, the bounds of the box represent the interquartile range, and the whiskers extend to 1.5× the interquartile range on either side of the median.

and primary tumor metabolism at various time points (pre-treatment, post-treatment, and variation) were detailed in [Figure S3](#). For systemic inflammatory markers, the pre-treatment BLR was positively correlated with the pre-treatment SLR, and Δ BLR% was positively correlated with both Δ SLR% and Δ NLR%. Various metabolic parameters of the primary tumor exhibited significant positive correlations with systemic inflammatory markers. Specifically, in the pre-treatment phase, MTV and TLG were positively correlated with the NLR, SLR, and BLR; in the post-treatment phase, the SUL_{max} , SUL_{mean} , SUL_{peak} , MTV, and TLG were positively correlated with the SLR; during the variation phase, Δ SUL_{max} %, Δ SUL_{mean} %, Δ SUL_{peak} %, and Δ TLG% were positively correlated with

Δ NLR%. Significant collinearity was observed among the primary tumor metabolic parameters.

Association between irAEs on PET/CT with MPR and pathologic regression

Of the 36 enrolled patients, 24 (66.7%) displayed at least one site of irAEs, including 10 (27.8%) with thyroiditis, 9 (25.0%) with pneumonitis, 8 (22.2%) with mediastinal granulomatous reaction, 4 (11.1%) with gastritis, 5 (13.9%) with colitis, 2 (5.6%) with osteo-articular inflammation, 2 (5.6%) with cutaneous inflammation, and 1 (2.8%) with pleuritis. Occurrence of irAEs on PET/CT did not have significant effects on both MPR and pathologic regression

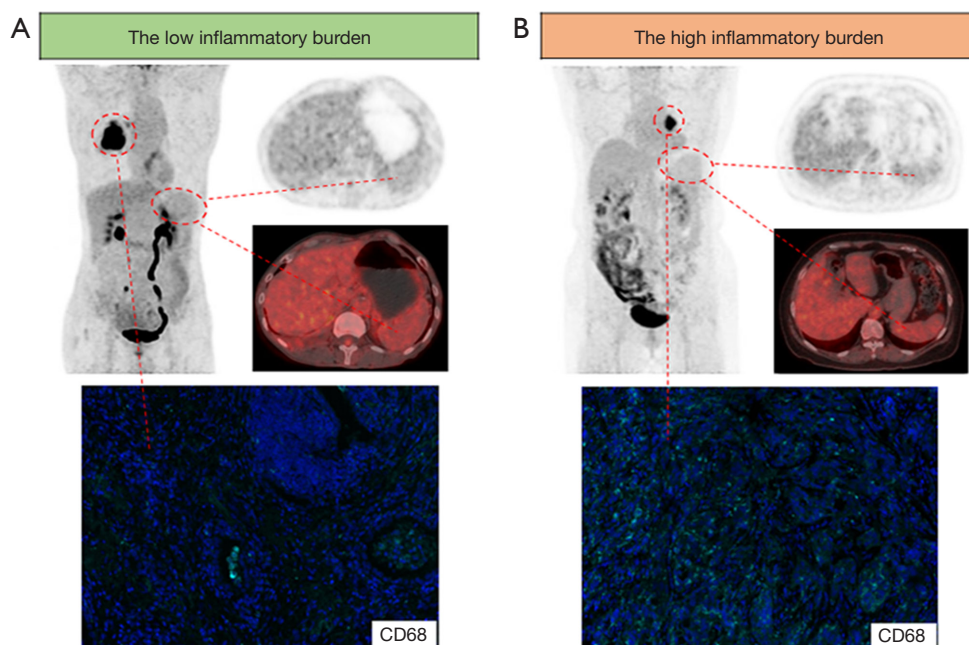


Figure 3 Representative PET/CT and pre-treatment CD68 staining images of patients with the low and high inflammatory burden. Immunofluorescence staining of CD68 at $\times 200$ magnification. Infiltration abundance was calculated by dividing the number of positively stained cells (green) by the total number of nuclear cells (blue). (A) Patient with the low inflammatory burden was a 67-year-old man with lung squamous cell carcinoma. The pre-treatment SLR = 0.80. Δ NLR% = -40.29%. The pre-treatment CD68⁺ macrophages infiltration abundance = 0.008%. Resection specimen showed this patient achieved MPR (95% of pathologic regression). This image is published with the patient's consent. (B) Patient with the high inflammatory burden was a 58-year-old woman with mixed lung squamous cell carcinoma and adenocarcinoma. The pre-treatment SLR = 0.88. Δ NLR% = 38.06%. The pre-treatment CD68⁺ macrophages infiltration abundance = 41.27%. Resection specimen showed this patient did not achieve MPR (40% of pathologic regression). This image is published with the patient's consent. PET/CT, positron emission tomography/computed tomography; SLR, spleen-to-liver ratio; NLR, neutrophil-to-lymphocyte ratio; MPR, major pathologic response.

in the overall and per-organ statistical analyses (Tables 4,5).

Discussion

This study provided a promising novel insight into the predictive value of longitudinal systemic inflammatory markers to stratify pathologic response to neoadjuvant immunotherapy. The main findings were as follows: first, Δ NLR% emerged as a significant negative predictor of MPR and negatively correlated with pathologic regression. Pre- and post-treatment SLRs were potential negative predictors of MPR and negatively correlated with pathologic regression. Second, the combination of pre-treatment SLR and Δ NLR% allowed oncologists to noninvasively classify patients into three groups, and patients in the high inflammatory burden group exhibiting the lowest pathologic regression showing the pre-treatment

immunosuppressive microenvironment with macrophage enrichment. Finally, the emergence of irAEs on PET/CT did not have significant effects on MPR and pathologic regression in the overall and per-organ analyses.

An elevated NLR indicates neutrophilia, lymphopenia, or both, physiologically indicating the relative absence of anti-tumor immunity (24). Studies have shown that the NLR was an important negative biomarker for the prediction and prognosis of immunotherapy response, as a high NLR (both pre- and post-treatment) and elevated NLR during variation were associated with poor clinical outcomes (10,15). In our study, Δ NLR% was a significant negative predictor of pathologic regression after neoadjuvant immunotherapy. Further analyses indicated that the dominant significant effect was attributable to the absolute neutrophil count (Δ). Studies have also supported the negative prognostic role of pre-treatment and variations in absolute neutrophil

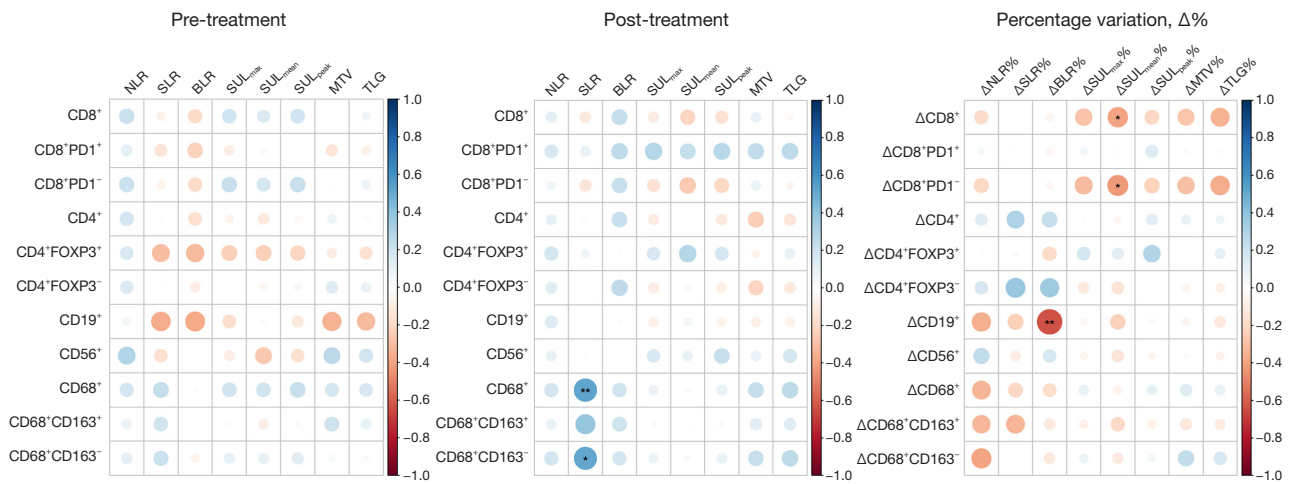


Figure 4 Correlation of tumor-infiltrating immune cells abundance with systemic inflammatory markers and primary tumor metabolism at various time points. *, P<0.05; **, P<0.01; Spearman's correlation. NLR, neutrophil-to-lymphocyte ratio; SLR, spleen-to-liver ratio; BLR, bone marrow-to-liver ratio; SUL, standardized uptake value corrected by lean body mass; MTV, metabolic tumor volume; TLG, total lesion glycolysis.

Table 4 Occurrence of irAEs on PET/CT with MPR

| irAEs on PET/CT | All patients (n=36) | Patients with MPR (n=13) | Patients without MPR (n=23) | P value |
|------------------------------------|---------------------|--------------------------|-----------------------------|---------|
| All organs | | | | 0.47 |
| Yes | 24 | 10 | 14 | |
| No | 12 | 3 | 9 | |
| Pneumonitis | | | | 0.44 |
| Yes | 9 | 2 | 7 | |
| No | 27 | 11 | 16 | |
| Thyroiditis | | | | 0.12 |
| Yes | 10 | 6 | 4 | |
| No | 26 | 7 | 19 | |
| Mediastinal granulomatous reaction | | | | 0.42 |
| Yes | 8 | 4 | 4 | |
| No | 28 | 9 | 19 | |
| Gastritis | | | | >0.99 |
| Yes | 4 | 1 | 3 | |
| No | 32 | 12 | 20 | |
| Colitis | | | | >0.99 |
| Yes | 5 | 2 | 3 | |
| No | 31 | 11 | 20 | |
| Other organs | | | | 0.14 |
| Yes | 5 | 0 | 5 | |
| No | 31 | 13 | 18 | |

All organs: refer to the occurrence of irAEs on PET/CT displayed at least one organ. Other organs: 2 patients had osteo-articular inflammation; 2 patients had cutaneous inflammation; 1 patient had pleuritis. irAEs, immune-related adverse events; PET/CT, positron emission tomography/computed tomography; MPR, major pathologic response.

Table 5 Occurrence of irAEs on PET/CT with pathologic regression

| irAEs on PET/CT | Pathologic regression (%), median [range] | P value |
|------------------------------------|---|---------|
| All organs | | 0.34 |
| Yes | 55 [0–100] | |
| No | 40 [5–100] | |
| Pneumonitis | | 0.57 |
| Yes | 30 [10–100] | |
| No | 45 [0–100] | |
| Thyroiditis | | 0.45 |
| Yes | 92.5 [0–100] | |
| No | 40 [5–100] | |
| Mediastinal granulomatous reaction | | 0.27 |
| Yes | 75 [10–100] | |
| No | 40 [0–100] | |
| Gastritis | | 0.54 |
| Yes | 37.5 [5–95] | |
| No | 47.5 [0–100] | |
| Colitis | | 0.97 |
| Yes | 40 [5–100] | |
| No | 45 [0–100] | |
| Other organs | | 0.06 |
| Yes | 20 [0–60] | |
| No | 50 [5–100] | |

All organs: refer to the occurrence of irAEs on PET/CT displayed at least one organ. Other organs: 2 patients had osteo-articular inflammation; 2 patients had cutaneous inflammation; 1 patient had pleuritis. irAEs, immune-related adverse events; PET/CT, positron emission tomography/computed tomography.

counts for immunotherapy (25,26). Recently, Kargl *et al.* (27) reported that neutrophils dominated the immune landscape of NSCLC; although many mechanisms were unknown, high levels of neutrophils were thought to be primarily involved in tumorigenesis and cancer proliferation and were responsible for treatment failure of immunotherapy (28).

Determining the role of lymphoid organ metabolism in immunotherapy has proven challenging because the results published to date have been inconclusive for various tumors and have not been fully studied in NSCLC. Our study showed a trend that higher pre- and post-treatment SLRs

appeared to be associated with poorer pathologic response, almost reaching statistical significance. This finding was consistent with those of previous studies demonstrating that a high SLR was associated with unfavorable patient outcomes (13,29). In contrast, Jin *et al.* (11) reported that an elevated SLR after immunotherapy was significantly correlated with longer survival. Lang *et al.* (12) proposed that a high BLR, rather than a high SLR, was associated with poor clinical outcomes. Some studies have also suggested that both a high SLR and BLR were associated with poor clinical outcomes (11,30,31). Indeed, the SLR and BLR presented a strong positive correlation (30), supporting the hypothesis of a pathophysiological mechanism and a common systemic inflammatory state throughout the whole body.

This exploratory study proposed a promising new method that combined the pre-treatment SLR and Δ NLR% to effectively stratify pathologic response to neoadjuvant immunotherapy in resectable NSCLC. This method emphasized the combined effect of peripheral blood tests and PET/CT scans in comprehensively assessing the host immune status and immune activation. Results showed that the high inflammatory burden group, characterized by a pre-treatment SLR >0.83 and Δ NLR% $>-17\%$, had the lowest pathologic regression and a pre-treatment TIME with CD68⁺ macrophages enrichment. There is persuasive evidence that macrophages promote cancer growth and malignant progression (32). Macrophages create a mutagenic and growth-promoting inflammatory environment during tumor initiation, stimulate angiogenesis, enhance tumor cell invasion, and suppress antitumor immunity during tumor progress (32). Therefore, the high inflammatory burden group exhibited CD68⁺ macrophages enrichment indicating an immunosuppressive microenvironment. The results provide complementary information for predictive markers, suggesting that in addition to the primary tumor, the host immune status also significantly influences the effect of immunotherapy. Notably, assessing host immune responses from peripheral blood alone can be unreliable because blood is susceptible to multiple factors, such as infection, steroid treatment, or other stress triggers. Our study specifically included lymphoid organ metabolism as an imaging marker of systemic inflammation and emphasized their combined effect. Both the pre- and post-treatment SLRs were potential negative predictors of pathologic response. Given the significant collinearity, we only included the pre-treatment SLR in the classification and did not include the post-treatment SLR. Moreover, post-immunotherapy

PET/CT scan is not mandatory in routine clinical practice despite the non-negligible significance. Recurrent PET/CT scans are not cost-effective and have problems with cumulative radiation doses. In summary, our study suggests that combining pre-treatment PET/CT scan with longitudinal peripheral blood tests can serve as promising tools for stratifying pathologic response to neoadjuvant immunotherapy in resectable NSCLC. This approach offers easy integration into clinical practice, involves no additional expenditure, and allows for straightforward calculations.

Theoretical evidence suggests the existence of crosstalk among tumor-infiltrating immune cells, circulating immune cells, and lymphatic organs (13,33). The spleen and bone marrow regulate the balance between the pro-tumoral circulating and infiltrating myeloid-derived suppressor cells and anti-tumoral-activated CD8⁺ T cells (13,34). Seban *et al.* (20) reported that a high baseline SLR was an independent factor for low stromal tumor-infiltrating lymphocytes with a significant negative correlation. They also found that an increased BLR was significantly associated with the upregulation of transcriptomic profiles, including regulatory T cell markers (30). Studies have shown that the spleen and bone marrow accumulated a large number of immunosuppressive cells, and a high SLR and BLR might represent the enriched mobilization of tumor-associated immunosuppressive cells, which migrated to the peripheral lymphoid organs and tumor sites and mediated a suppressive immune microenvironment (35-37). In our study, the high inflammatory burden group represented a pre-treatment immunosuppressive TIME with CD68⁺ macrophages enrichment, in consistency with previous studies of high SLR- and high NLR-mediated immunosuppressive TIMEs (20,24,38). Furthermore, blood and PET/CT imaging comprehensively assessed systemic inflammation status from different perspectives of peripheral circulating cells and organs metabolism. Significant positive correlations between blood and PET/CT inflammatory markers have been reported in several studies (31,39,40), suggesting the potential of diffuse spleen and bone marrow uptake as integrated imaging-derived biomarkers reflecting hematologic imbalance. In this study, other than the significant positive correlation between Δ NLR% and Δ BLR%, the correlation analyses between blood and PET/CT inflammatory markers were not significant, which may be due to the limited sample size. A larger sample size may yield statistically significant results. In addition, Wang *et al.* (41) demonstrated significant correlations between primary tumor metabolic parameters and various immune

cells in the TIME. Our results showed that the Δ SUL_{mean}% was negatively correlated with Δ CD8⁺ and Δ CD8⁺PD1⁻ T cells. Although these correlations remain uncertain, they may reveal the potential of tumor and lymphoid tissue metabolism to characterize the information of tumor-infiltrating immune cells in the TIME. Advanced radiomic methods based on PET/CT texture analysis will be used to characterize the landscape of the tumor microenvironment in future studies.

PET/CT is an effective imaging method for the early detection of potential irAEs before clinical diagnosis with high detection rates among multiple imaging modalities, regardless of whether the patient is symptomatic or not (42,43). In our study, 24 patients (66.7%) had at least one site of irAEs on PET/CT, with thyroiditis being the most common manifestation. Studies have reported that clinical irAEs are related to the anti-tumor effects, with better efficacy and longer survival rates (14,44,45). However, the value of irAEs detected by PET/CT has been poorly investigated. Humbert *et al.* (21) demonstrated that immune-induced gastritis on PET/CT was a novel and strong imaging biomarker of improved overall survival. However, the emergence of irAEs on PET/CT did not have significant effects on both MPR and pathologic regression in the overall and per-organ statistical analyses in our study. The relatively short interval between pre- and post-treatment PET/CT scans (approximately 1 month) might be insufficient to detect delayed organ inflammation uptake, as most irAEs occurred during the first 3 months.

There are some limitations in this study. First, this was a single-center retrospective analysis of prospectively acquired data from a phase Ib trial. The preliminary and exploratory study had a limited sample size, and not all biopsy tumor tissues were available. Second, the small sample size posed challenges for comprehensive analyses of histological subgroups. Finally, we did not evaluate the long-term clinical endpoints such as progression-free survival and overall survival, as our study focused on pathologic response and MPR, which is a vital short-term endpoint that has potential to replace survival outcomes in neoadjuvant immunotherapy setting. Future studies with large sample sizes, long-term follow-up, and comprehensive evaluation are warranted to provide more conclusive insights.

Conclusions

In conclusion, the combination of systemic inflammatory markers from pre-treatment PET/CT scan and longitudinal

peripheral blood tests are promising tools for stratifying pathologic response to resectable NSCLC in neoadjuvant immunotherapy, providing an easily integrable approach in routine clinical practice to help patients selection with potential benefits. The high inflammatory burden group showed the lowest pathologic regression and the pre-treatment immunosuppressive microenvironment with macrophage enrichment. Our findings may serve as preliminary data to encourage prospective studies to further explore the pathophysiological mechanisms involving systemic inflammatory markers and their association with the TIME and clinical outcomes.

Acknowledgments

We thank the patients and their families, and the participating study teams for making this study possible.

Funding: This work was supported by the National Natural Science Foundation of China (No. 82001870).

Footnote

Reporting Checklist: The authors have completed the TRIPOD reporting checklist. Available at <https://tclr.amegroups.com/article/view/10.21037/tlcr-24-598/rc>

Data Sharing Statement: Available at <https://tclr.amegroups.com/article/view/10.21037/tlcr-24-598/dss>

Peer Review File: Available at <https://tclr.amegroups.com/article/view/10.21037/tlcr-24-598/prf>

Conflicts of Interest: All authors have completed the ICMJE uniform disclosure form (available at <https://tclr.amegroups.com/article/view/10.21037/tlcr-24-598/coif>). The authors have no conflicts of interest to declare.

Ethical Statement: The authors are accountable for all aspects of the work in ensuring that questions related to the accuracy or integrity of any part of the work are appropriately investigated and resolved. The study was conducted in accordance with the Declaration of Helsinki (as revised in 2013). The Ethics Committee and Institutional Review Board of the National Cancer Center/Cancer Hospital, Chinese Academy of Medical Sciences and Peking Union Medical College approved this prospective study (No. 17-151/1407), and informed consent was obtained from all individual participants.

Open Access Statement: This is an Open Access article distributed in accordance with the Creative Commons Attribution-NonCommercial-NoDerivs 4.0 International License (CC BY-NC-ND 4.0), which permits the non-commercial replication and distribution of the article with the strict proviso that no changes or edits are made and the original work is properly cited (including links to both the formal publication through the relevant DOI and the license). See: <https://creativecommons.org/licenses/by-nc-nd/4.0/>.

References

1. Nasim F, Sabath BF, Eapen GA. Lung Cancer. *Med Clin North Am* 2019;103:463-73.
2. Forde PM, Chaft JE, Smith KN, et al. Neoadjuvant PD-1 Blockade in Resectable Lung Cancer. *N Engl J Med* 2018;378:1976-86.
3. Gao S, Li N, Gao S, et al. Neoadjuvant PD-1 inhibitor (Sintilimab) in NSCLC. *J Thorac Oncol* 2020;15:816-26.
4. Chaft JE, Oezkan F, Kris MG, et al. Neoadjuvant atezolizumab for resectable non-small cell lung cancer: an open-label, single-arm phase II trial. *Nat Med* 2022;28:2155-61.
5. Eichhorn F, Klotz LV, Kriegsmann M, et al. Neoadjuvant anti-programmed death-1 immunotherapy by pembrolizumab in resectable non-small cell lung cancer: First clinical experience. *Lung Cancer* 2021;153:150-7.
6. Mantovani A, Allavena P, Sica A, et al. Cancer-related inflammation. *Nature* 2008;454:436-44.
7. Roxburgh CS, McMillan DC. Cancer and systemic inflammation: treat the tumour and treat the host. *Br J Cancer* 2014;110:1409-12.
8. Munn LL. Cancer and inflammation. *Wiley Interdiscip Rev Syst Biol Med* 2017;9:10.1002/wsbm.1370.
9. Hanahan D, Weinberg RA. Hallmarks of cancer: the next generation. *Cell* 2011;144:646-74.
10. Platini H, Ferdinand E, Kohar K, et al. Neutrophil-to-Lymphocyte Ratio and Platelet-to-Lymphocyte Ratio as Prognostic Markers for Advanced Non-Small-Cell Lung Cancer Treated with Immunotherapy: A Systematic Review and Meta-Analysis. *Medicina (Kaunas)* 2022;58:1069.
11. Jin P, Bai M, Liu J, et al. Tumor metabolic and secondary lymphoid organ metabolic markers on 18F-fludeoxyglucose positron emission tomography predict prognosis of immune checkpoint inhibitors in advanced lung cancer. *Front Immunol* 2022;13:1004351.
12. Lang D, Ritzberger L, Rambousek V, et al. First-Line

- Pembrolizumab Mono- or Combination Therapy of Non-Small Cell Lung Cancer: Baseline Metabolic Biomarkers Predict Outcomes. *Cancers (Basel)* 2021;13:6096.
13. Seban RD, Assié JB, Giroux-Leprieur E, et al. Prognostic value of inflammatory response biomarkers using peripheral blood and 18F-FDG PET/CT in advanced NSCLC patients treated with first-line chemo- or immunotherapy. *Lung Cancer* 2021;159:45-55.
 14. Grangeon M, Tomasini P, Chaleat S, et al. Association Between Immune-related Adverse Events and Efficacy of Immune Checkpoint Inhibitors in Non-small-cell Lung Cancer. *Clin Lung Cancer* 2019;20:201-7.
 15. Guo Y, Xiang D, Wan J, et al. Focus on the Dynamics of Neutrophil-to-Lymphocyte Ratio in Cancer Patients Treated with Immune Checkpoint Inhibitors: A Meta-Analysis and Systematic Review. *Cancers (Basel)* 2022;14:5297.
 16. Gajewski TF, Schreiber H, Fu YX. Innate and adaptive immune cells in the tumor microenvironment. *Nat Immunol* 2013;14:1014-22.
 17. Tao X, Li N, Wu N, et al. The efficiency of (18)F-FDG PET-CT for predicting the major pathologic response to the neoadjuvant PD-1 blockade in resectable non-small cell lung cancer. *Eur J Nucl Med Mol Imaging* 2020;47:1209-19.
 18. Prigent K, Lasnon C, Ezine E, et al. Assessing immune organs on (18)F-FDG PET/CT imaging for therapy monitoring of immune checkpoint inhibitors: inter-observer variability, prognostic value and evolution during the treatment course of melanoma patients. *Eur J Nucl Med Mol Imaging* 2021;48:2573-85.
 19. Seban RD, Moya-Plana A, Antonios L, et al. Prognostic 18F-FDG PET biomarkers in metastatic mucosal and cutaneous melanoma treated with immune checkpoint inhibitors targeting PD-1 and CTLA-4. *Eur J Nucl Med Mol Imaging* 2020;47:2301-12.
 20. Seban RD, Rouzier R, Latouche A, et al. Total metabolic tumor volume and spleen metabolism on baseline [18F]-FDG PET/CT as independent prognostic biomarkers of recurrence in resected breast cancer. *Eur J Nucl Med Mol Imaging* 2021;48:3560-70.
 21. Humbert O, Bauckneht M, Gal J, et al. Prognostic value of immunotherapy-induced organ inflammation assessed on (18)FDG PET in patients with metastatic non-small cell lung cancer. *Eur J Nucl Med Mol Imaging* 2022;49:3878-91.
 22. Ling Y, Li N, Li L, et al. Different pathologic responses to neoadjuvant anti-PD-1 in primary squamous lung cancer and regional lymph nodes. *NPJ Precis Oncol* 2020;4:32.
 23. Wang S, Yuan P, Mao B, et al. Genomic features and tumor immune microenvironment alteration in NSCLC treated with neoadjuvant PD-1 blockade. *NPJ Precis Oncol* 2022;6:2.
 24. Gabrilovich DI, Nagaraj S. Myeloid-derived suppressor cells as regulators of the immune system. *Nat Rev Immunol* 2009;9:162-74.
 25. Murakami Y, Tamiya A, Taniguchi Y, et al. Retrospective analysis of long-term survival factors in patients with advanced non-small cell lung cancer treated with nivolumab. *Thorac Cancer* 2022;13:593-601.
 26. Sibille A, Henket M, Corhay JL, et al. White Blood Cells in Patients Treated with Programmed Cell Death-1 Inhibitors for Non-small Cell Lung Cancer. *Lung* 2021;199:549-57.
 27. Kargl J, Busch SE, Yang GH, et al. Neutrophils dominate the immune cell composition in non-small cell lung cancer. *Nat Commun* 2017;8:14381.
 28. Coffelt SB, Wellenstein MD, de Visser KE. Neutrophils in cancer: neutral no more. *Nat Rev Cancer* 2016;16:431-46.
 29. Sachpekidis C, Weru V, Kopp-Schneider A, et al. The prognostic value of [18F]FDG PET/CT based response monitoring in metastatic melanoma patients undergoing immunotherapy: comparison of different metabolic criteria. *Eur J Nucl Med Mol Imaging* 2023;50:2699-714.
 30. Seban RD, Nemer JS, Marabelle A, et al. Prognostic and theranostic 18F-FDG PET biomarkers for anti-PD1 immunotherapy in metastatic melanoma: association with outcome and transcriptomics. *Eur J Nucl Med Mol Imaging* 2019;46:2298-310.
 31. Lee JH, Lee HS, Kim S, et al. Prognostic significance of bone marrow and spleen (18)F-FDG uptake in patients with colorectal cancer. *Sci Rep* 2021;11:12137.
 32. Qian BZ, Pollard JW. Macrophage diversity enhances tumor progression and metastasis. *Cell* 2010;141:39-51.
 33. Morrison SJ, Scadden DT. The bone marrow niche for haematopoietic stem cells. *Nature* 2014;505:327-34.
 34. Groth C, Hu X, Weber R, et al. Immunosuppression mediated by myeloid-derived suppressor cells (MDSCs) during tumour progression. *Br J Cancer* 2019;120:16-25.
 35. Haverkamp JM, Crist SA, Elzey BD, et al. In vivo suppressive function of myeloid-derived suppressor cells is limited to the inflammatory site. *Eur J Immunol* 2011;41:749-59.
 36. Kumar V, Patel S, Tcyganov E, et al. The Nature of Myeloid-Derived Suppressor Cells in the Tumor Microenvironment. *Trends Immunol* 2016;37:208-20.

37. Cortez-Retamozo V, Etzrodt M, Newton A, et al. Origins of tumor-associated macrophages and neutrophils. *Proc Natl Acad Sci U S A* 2012;109:2491-6.
38. Levy L, Mishalian I, Bayuch R, et al. Splenectomy inhibits non-small cell lung cancer growth by modulating anti-tumor adaptive and innate immune response. *Oncoimmunology* 2015;4:e998469.
39. Yoon HJ, Kim BS, Moon CM, et al. Prognostic value of diffuse splenic FDG uptake on PET/CT in patients with gastric cancer. *PLoS One* 2018;13:e0196110.
40. Nam HY, Kim SJ, Kim IJ, et al. The clinical implication and prediction of diffuse splenic FDG uptake during cancer surveillance. *Clin Nucl Med* 2010;35:759-63.
41. Wang Y, Zhao N, Wu Z, et al. New insight on the correlation of metabolic status on (18)F-FDG PET/CT with immune marker expression in patients with non-small cell lung cancer. *Eur J Nucl Med Mol Imaging* 2020;47:1127-36.
42. Mekki A, Dercle L, Lichtenstein P, et al. Detection of immune-related adverse events by medical imaging in patients treated with anti-programmed cell death 1. *Eur J Cancer* 2018;96:91-104.
43. Iravani A, Osman MM, Wepler AM, et al. FDG PET/CT for tumoral and systemic immune response monitoring of advanced melanoma during first-line combination ipilimumab and nivolumab treatment. *Eur J Nucl Med Mol Imaging* 2020;47:2776-86.
44. Kotwal A, Kottschade L, Ryder M. PD-L1 Inhibitor-Induced Thyroiditis Is Associated with Better Overall Survival in Cancer Patients. *Thyroid* 2020;30:177-84.
45. Nobashi T, Baratto L, Reddy SA, et al. Predicting Response to Immunotherapy by Evaluating Tumors, Lymphoid Cell-Rich Organs, and Immune-Related Adverse Events Using FDG-PET/CT. *Clin Nucl Med* 2019;44:e272-9.

Cite this article as: Tao X, Zhang Q, Yuan P, Wang S, Ying J, Li N, Guo W, Li J, Guo L, Liu Y, Zhang Z, Zhao S, Gao S, Wu N. Predictive value of longitudinal systemic inflammatory markers for pathologic response to neoadjuvant PD-1 blockade in resectable non-small cell lung cancer. *Transl Lung Cancer Res* 2024;13(11):2972-2986. doi: 10.21037/tlcr-24-598